Mechanical and Histological Characteristics of Phasix™ ST Mesh in a Porcine Model of Hernia Repair

Corey R. Deeken , Darcy H. Gagne & Amit Badhwar

Published online: 12 Oct 2020.

Submit your article to this journal ☑

Article views: 316

View related articles ☑

View Crossmark data ☑

Citing articles: 1 View citing articles ☑

Taylor & Francis
Taylor & Francis Group

ORIGINAL RESEARCH

🔓 OPEN ACCESS Check for updates

Mechanical and Histological Characteristics of Phasix™ ST Mesh in a Porcine Model of Hernia Repair

Corey R. Deeken[a] 🄳, Darcy H. Gagne[b], and Amit Badhwar[b]

[a]Covalent Bio LLC, Eureka, Missouri, USA; [b]Becton, Dickinson and Company (BD), Warwick, Rhode Island, USA

ABSTRACT

Purpose: The objective of this study was to determine mechanical and histological properties of Phasix™ ST Mesh in various defect sizes and characterize the tissue replacing Phasix™ ST Mesh in a porcine model of ventral hernia repair.

Methods: Simulated hernia defects were surgically created in the midline of twenty-four (n = 24) Yucatan pigs. Treatment groups included 8 cm defect sutured closed (buttress) and unclosed 4 cm and 8 cm defect groups. Phasix™ ST Mesh (15 cm diameter circle) was implanted laparoscopically and fixated circumferentially with SorbaFix™ Absorbable Fixation System fasteners. The repair sites underwent mechanical, molecular weight, and histological evaluation at 48 and 72 weeks postimplantation.

Results: Mechanical testing of Phasix™ ST Mesh-repaired sites revealed similar strengths at both time points for all three repair types, $p > 0.05$ in all cases (48 weeks: 142.4 ± 6.0 N, 142.3 ± 16.5 N, and 168.8 ± 38.5 N; 72 weeks: 110.0 ± 18.3 N, 138.6 ± 42.2 N, and 160.6 ± 42.0 N for 4 cm defect, 8 cm defect, and 8 cm buttress, respectively. mean ± SEM) No significant differences were observed over time except at 72 weeks postimplantation when the 4 cm defect group exhibited significantly lower strength than the T_0 strength of Phasix™ ST Mesh (204.6 ± 5.0 N, $p < 0.05$). The molecular weight of Phasix™ ST Mesh decreased over time, regardless of repair type. Histological analysis showed comparable mature collagen/fibrovascular tissue around and within the Phasix™ ST Mesh interstices, including the segment of mesh overlying the defect.

Conclusion: Phasix™ ST Mesh-repaired sites exhibited similar mechanical strengths and histological properties across all defect sizes in this porcine model.

Introduction

Over the past several decades, the field of hernia repair has been influenced by significant advancements in both surgical technique and biomaterials utilized to reconstruct the abdominal wall. In the 1940s, silver and tantalum meshes were introduced for hernia repair applications [1,2], and by the late-1950s, permanent synthetic polymer meshes were utilized [3]. In the decades following, more than 150 unique designs have been developed, comprised of permanent synthetic polymers, biological tissue-derived materials, and most recently, resorbable polymers [4,5].

Several resorbable hernia repair devices are now available with a variety of mechanical characteristics and resorption profiles. Devices in this category are comprised of: poly-4-hydroxybutyrate (Phasix™ Mesh, Becton, Dickinson and Company (BD), Franklin Lakes, NJ), ultra-pure fibroin derived from silk (Seri® Surgical Scaffold, Sofregen Medical), polyglycolic acid (Safil® Mesh, B Braun), a co-polymer of glycolide and lactide (Dexon™ Mesh, Covidien & Vicryl™ Knitted Mesh, Ethicon, Inc.), a co-polymer of polyglycolic acid and trimethylene carbonate (Gore® Bio-A® Tissue Reinforcement, W.L. Gore & Assoc., Inc.), and a co-polymer of glycolide, lactide, and trimethylene carbonate (TIGR® Matrix Surgical Mesh, Insightra Medical) [4,5].

A unique, fully-resorbable composite mesh design launched in 2015 (Phasix™ ST Mesh, Becton, Dickinson and Company (BD), Franklin Lakes, NJ) and is depicted in Figure 1. Phasix™ ST Mesh is comprised of fully resorbable, biologically-derived, poly-4-hydroxybutyrate (P4HB) monofilament that is co-knitted with polyglycolic acid (PGA) and coated with a resorbable hydrogel layer on the visceral side of the mesh [6]. The hydrogel layer is comprised of sodium hyaluronate (HA), carboxymethylcellulose (CMC), and polyethylene glycol (PEG). The hydrogel provides a barrier to minimize visceral tissue attachment and resorbs in approximately 30 days, while the underlying P4HB mesh serves as a scaffold for tissue ingrowth and mechanical support for the repair, resorbing gradually over a period of 12–18 months [6].

In a preclinical study, Phasix™ ST Mesh was implanted in an intraperitoneal (underlay) fashion in a porcine model
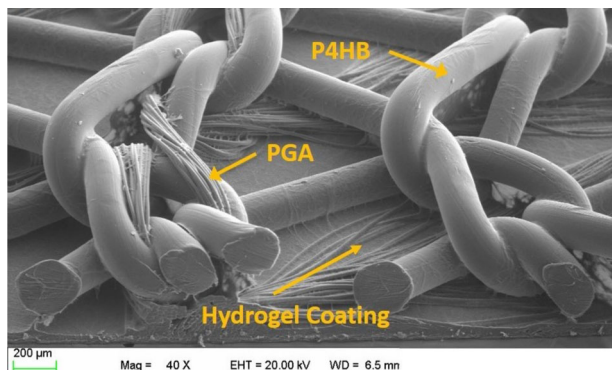
Figure 1. Scanning electron micrograph (SEM) of Phasix™ ST Mesh (40× magnification; scale bar = 200 µm). Phasix™ ST Mesh is comprised of fully resorbable poly-4-hydroxybutyrate (P4HB) fibers co-knitted with polyglycolic acid (PGA) and coated with a resorbable hydrogel layer on the visceral side of the mesh. The hydrogel layer is comprised of sodium hyaluronate (HA), carboxymethylcellulose (CMC), and polyethylene glycol (PEG).

of ventral hernia repair [7]. Phasix™ ST Mesh-repaired sites exhibited similar postimplantation strength and histological characteristics as partially resorbable (Ventralight™ ST Mesh) and fully resorbable (Phasix™ Mesh) meshes at 12 and 24 weeks postimplantation. The strength of Phasix™ ST Mesh-repaired sites remained stable throughout the study and significantly greater ($p < 0.05$) than both the preimplantation strength of Phasix™ ST Mesh itself and the native abdominal wall. Histological analysis showed a mild inflammatory response and a minimal to mild fibrosis and neovascularization associated with Phasix™ ST Mesh-repaired sites at 12 and 24 weeks postimplantation. Taken together, these results demonstrated that Phasix™ ST Mesh, along with newly deposited host tissue, augmented the strength of the native abdominal wall, despite active resorption of the P4HB fibers comprising the mesh.

As an extension of that work, the objective of the current study was to compare the mechanical and histological properties of Phasix™ ST Mesh in various defect sizes and characterize the tissue replacing Phasix™ ST Mesh in a similar porcine model of ventral hernia repair at 48 and 72 weeks postimplantation.

Methods

Study compliance

This study was reviewed by the Institutional Animal Care and Use Committee (IACUC) of CBSET, Inc. (Lexington, MA), and was conducted in compliance with all regulations regarding humane treatment of laboratory animals.

Study design

The study population consisted of n = 27 female (nulliparous and non-pregnant) Yucatan swine (48.2–60.3 kg at implantation): n = 24 study animals and n = 3 designated replacement animals. The animals were divided equally between three treatment groups (n = 8 each), which included an 8 cm defect, sutured closed (buttress group) and unclosed 4 cm and 8 cm defect groups. In all three groups,

Phasix™ ST Mesh was implanted and fixated using SorbaFix™ Absorbable Fixation System fasteners in a double crown technique.

Perioperative preparation of animals

Animals were not offered their daily food ration prior to surgical induction to decrease the chances of perioperative regurgitation. Water was not restricted. Daily food ration was provided upon recovery from anesthesia; thus, no daily food ration was omitted. On the morning of surgery, Carprofen (∼2.2 mg/kg, oral [PO]) was administered. Telazol® (4–6 mg/kg, intramuscular [IM]) was administered as a pre-anesthetic. Isoflurane anesthesia (delivered in 100% oxygen) was administered to effect via mask/nosecone until the animals were in a plane of anesthesia that facilitated endotracheal intubation. Once sufficiently anesthetized, the animals were intubated and maintained with isoflurane inhalant anesthetic to effect for the remainder of the surgical procedure. An intravenous (IV) catheter was placed in a peripheral vein for administration of supportive IV fluids. Preemptive buprenorphine therapy (0.03 mg/kg, IM) was administered; additionally, antibiotic therapy (Ceftiofur [5 mg/kg, IM] and Excede® [5 mg/kg, IM]) was administered at time of anesthesia, prior to surgical incision. An ophthalmic lubricant was applied to the eyes. The animals were prepared for surgery using accepted veterinary care standards. The hair was shaved from the abdominal region, and the animal was placed in dorsal recumbency. Supportive fluids (Lactated Ringer's Solution) were administered, and the fluid volume was documented in the animal's record. Warm water heating pads and/or other warming devices were used to maintain adequate body temperature while under anesthesia. The animals were prepared and appropriately draped for aseptic procedures.

Surgical procedures

A midline incision (20 cm) was made through the skin over the linea alba, leaving the peritoneal layer intact around the umbilicus. The aponeurosis of the rectus abdominus was identified and incised bilaterally adjacent to the umbilicus, leaving the peritoneum intact. Blunt dissection was used to separate the underlying muscle to create a defect of either 4 or 8 cm in length, depending on treatment group. Immediately after surgical creation, the dimensions (i.e., length and width) of the defect were measured with a sterile ruler and recorded. An image of the defect with a ruler in plane was taken for morphometric analysis. The animals were divided equally between three treatment groups, which included an 8 cm defect sutured closed (buttress group) and unclosed 4 cm and 8 cm defect groups (Figure 2). In the 8 cm buttress group, the defect was closed with 2-0 PDS™ sutures, while in the 4 cm and 8 cm defect groups, the defect remained open.

Carbon dioxide insufflation was established with the use of a Verres needle introduced into the peritoneal cavity. Intra-abdominal pressure was maintained at approximately
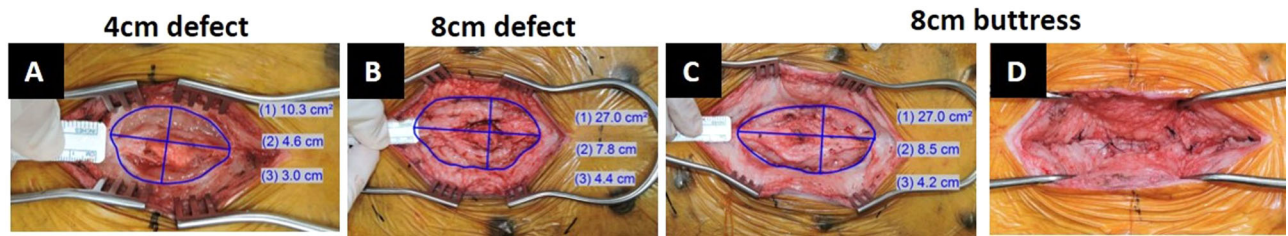
Figure 2. Simulated hernia defects surgically created in the midline of Yucatan pigs: (A) 4 cm defect group, unclosed; (B) 8 cm defect group, unclosed; (C) 8 cm buttress group prior to closure; and (D) 8 cm buttress group after closure.

10–12 mmHg. Three trocars were placed through approximately 1–2 cm incisions to accommodate a laparoscope and instrumentation. The typical trocar placement was one on either side of the abdomen and one trocar on the midline (subxiphoid).

A sterile template was utilized to mark the intended locations of each fastener and the center of the defect directly on each mesh. Phasix^{TM} ST Mesh (15 cm diameter circle) was then hydrated for 1–3 seconds in sterile 0.9% sodium chloride, implanted laparoscopically, and fixated circumferentially with approximately 40 SorbaFix^{TM} Absorbable Fixation System fasteners in a double crown configuration (Figure 3). SorbaFix^{TM} Absorbable Fixation System fasteners were utilized in accordance with the product Instructions for Use [8]. Bupivacaine was infused into the incision and trocar sites (not to exceed 2 mg/kg), and the trocar sites were closed with absorbable suture using standard closure techniques. The midline was closed using standard suture techniques. Suture passer sites were closed with tissue glue. Buprenorphine (0.02 mg/kg, IM) and Carprofen (approximately ∼2.2–4.4 mg/kg, PO) were generally administered every 11 hours ± 1 hour up to 72 hours post-procedure. Analgesics were continued as needed based on clinical assessment by the veterinary staff. Animal health (i.e., incision site, implant site, and clinical observations), body weights/condition, and clinical pathology were monitored at predetermined, regular intervals.

Animals were euthanized at 48 weeks (336 ± 3 days, 80.0–106.0 kg at explantation) and 72 weeks (504 ± 3 days, 91.0–131.0 kg at explantation), and a limited necropsy was performed. The abdominal skin was dissected from the abdomen, and the abdominal wall was reflected back to visualize the defect region, preserving any peritoneal tissue attachments. After the region was examined, the defect site with surrounding native abdominal wall (NAW) tissue was excised and placed in saline solution (0.9% sodium chloride) for subsequent mechanical testing, molecular weight analysis, and histological evaluation.

Mechanical testing

The explanted tissues were placed on ice packs and shipped to the mechanical testing facility along with non-implanted (T$_0$) meshes surrounded by moistened gauze and placed on ice packs. Specimens were refrigerated overnight and brought to room temperature prior to testing the following day. Non-adherent tissue was removed as needed without interfering with the embedded device. Ball burst testing was
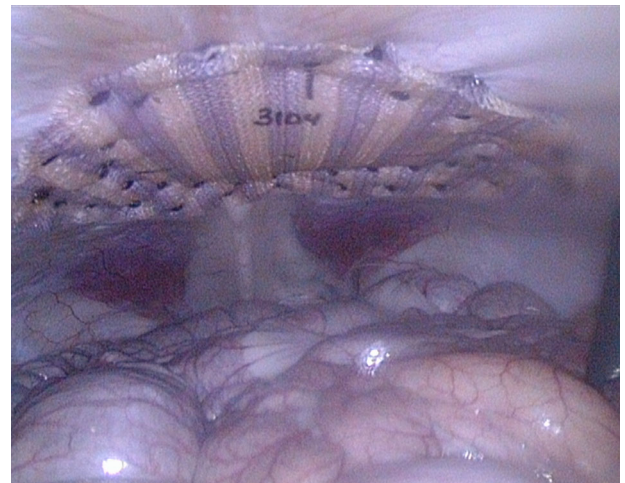

Figure 3. 4 cm unclosed repair immediately after defect closure and fixation of mesh using SorbaFix^{TM} Absorbable Fixation System fasteners in a double crown technique.

performed directly over the surgical defect site using an Instron® load frame with an Instron® 2 kN load cell. A test fixture was utilized to secure each device between two polymer plates, each covered with 120-grit sandpaper. The surgical defect site was centered in the 11 mm diameter hole of the fixture, and a 9.5 mm diameter ball was applied in compression at a rate of 25.4 mm/min, with a data acquisition frequency of 20 Hz. The peak ball burst force was recorded for each specimen and compared to the preimplantation (T$_0$) strength of Phasix^{TM} ST Mesh. Following burst testing, each specimen was bisected. One half was sent for molecular weight analysis, while the other half was placed into 10% neutral buffered formalin for histological analysis.

Gel permeation chromatography (GPC) analysis

Mesh-tissue explants were manually cleaned and enzymatically digested to remove residual tissue prior to Gel Permeation Chromatography (GPC) analysis as described previously [9,10]. Briefly, explants were placed in 50 mL tubes containing 25 mL collagenase (type I) solution (1.0 mg/mL) in TESCA buffer (50 mM 2-[Tris(hydroxymethyl)methylamino]-1-ethane-sulfonic acid, 2 mM calcium chloride, 10 mM sodium azide, pH 7.4). The tubes were placed in a shaker/incubator at 50 rpm at 37 °C to digest the tissue. After overnight incubation (∼17 hours), the samples were removed from the buffer and manually cleaned of tissue. The cleaned meshes were rinsed in

Table 1. Morphometric evaluation of defect area, length, and width demonstrating successful creation of consistent surgical defects.

Mean ± Std Dev	4cm defect		8cm defect		8cm buttress	
	48 weeks	72 weeks	48 weeks	72 weeks	48 weeks	72 weeks
Defect Area (cm^2)	11.1 ± 2.1	10.2 ± 1.7	35.3 ± 5.2	27.5 ± 8.2	35.2 ± 7.4	29.4 ± 1.9
Length (cm)	4.9 ± 0.8	4.7 ± 0.3	9.0 ± 0.6	8.2 ± 0.7	8.6 ± 1.0	8.5 ± 0.7
Width (cm)	3.1 ± 0.3	3.0 ± 0.4	5.4 ± 0.4	4.3 ± 1.0	5.6 ± 0.7	4.9 ± 0.5

distilled water, followed by 70% ethanol, and dried prior to GPC analysis. Cleaned mesh samples were dissolved at 1 mg/mL in chloroform containing an internal standard for retention time. Then, 95 μL was injected onto a GPC column, and GPC analysis was performed in chloroform at 1 mL/min using a Tosoh HPLC with RI detector fitted with a Polymer Labs PLgel column (5 microns, mixed C, 300×7.5 mm). Calibration was performed against monodisperse polystyrene standards. The molecular weight of each mesh explant was measured once per explant and reported as mean kDa ± standard deviation.

Histological evaluation

The implant site tissue samples were trimmed to yield one cross-section at the center of the defect-mesh interface, as well as cross-sections to the left and right of the defect-mesh interface. Specimens were processed, embedded, and sectioned at approximately 5 μm to yield Hematoxylin and Eosin (H&E), Masson's Trichrome (MT), and Picrosirius Red (PSR) stained slides for each specimen. Light microscopy was utilized to characterize the host response, including inflammation, fibrosis, collagen deposition/content, and vascularity/vascular integration.

Histological parameters were scored according to the following established [9,11,12] histomorphology scoring matrix:

0 = No response
1 = Minimal/barely detectable
2 = Mild/slightly detectable
3 = Moderate/easily detectable
4 = Marked/very evident

PSR stained slides were evaluated using polarized light microscopy. Newly deposited, immature (type III) collagen fibers appear green, while mature (type I) collagen fibers appear orange-red.

Collagen morphology was scored according to the following matrix [9]:

1 = Green (thin fibers) predominant
2 = Mixed
3 = Orange-red (thick fibers) predominant

Statistical analyses

Data were analyzed and graphically displayed using GraphPad Prism® 6.0 statistical software (GraphPad Software Inc., La Jolla, CA). A non-parametric, Kruskal-Wallis test with Dunn's post-test was performed with statistical significance set at $p < 0.05$. Ball burst strength is presented as mean ± standard error of the mean, molecular weight is presented as mean ± standard deviation, and histomorphological parameters are presented as median score.

Results

There was no mortality as a result of this study, and data from designated replacement animals were not utilized in any analyses. Eight animals (n = 8) were euthanized from each of three treatment groups, including an 8 cm defect, sutured closed (buttress group) and unclosed 4 cm and 8 cm defect groups. Macroscopically, there were omental tissue attachments at both time points, regardless of the defect type or size, without any other relevant, macroscopic findings. When evaluated morphometrically, the defect area, length, and width were similar between the 48 and 72 week groups for all defect sizes/types evaluated (Table 1), demonstrating successful creation of consistent surgical defects.

Mechanical testing

After collagenase digestion of native host tissue, Phasix^{TM} ST Mesh remained intact at 48 weeks, but only fragments of low molecular weight mesh remained at 72 weeks postimplantation (Figure 4). Mechanical testing of Phasix^{TM} ST Mesh-repaired sites revealed similar strengths at both time points for all three repair types, $p > 0.05$ in all cases (48 weeks: 142.4 ± 6.0 N, 142.3 ± 16.5 N, and 168.8 ± 38.5 N; 72 weeks: 110.0 ± 18.3 N, 138.6 ± 42.2 N, and 160.6 ± 42.0 N for 4 cm defect, 8 cm defect, and 8 cm buttress, respectively (mean ± standard error of the mean) (Figure 5). No significant differences were observed over time except at 72 weeks postimplantation when the 4 cm defect group exhibited significantly lower strength than the T_0 strength of Phasix^{TM} ST Mesh (204.6 ± 5.0 N, $p < 0.05$). At all time points and defect sizes investigated, the strength of the repair met or exceeded the 72 N threshold previously recommended by Deeken and Matthews [13].

Gel permeation chromatography (GPC) analysis

The molecular weight of Phasix^{TM} ST Mesh decreased over time in all groups, regardless of repair type (Figure 6). Prior to implantation (T_0), the molecular weight of Phasix^{TM} ST Mesh was 336 ± 3.7 kDa. At 48 weeks postimplantation, the molecular weight decreased to 47 ± 3.7, 45 ± 3.3, and 47 ± 2.4 kDa for the 4 cm defect, 8 cm defect, and 8 cm buttress groups, respectively. Similarly, at 72 weeks postimplantation, the molecular weight decreased to 20 ± 1.3, 20 ± 1.5,
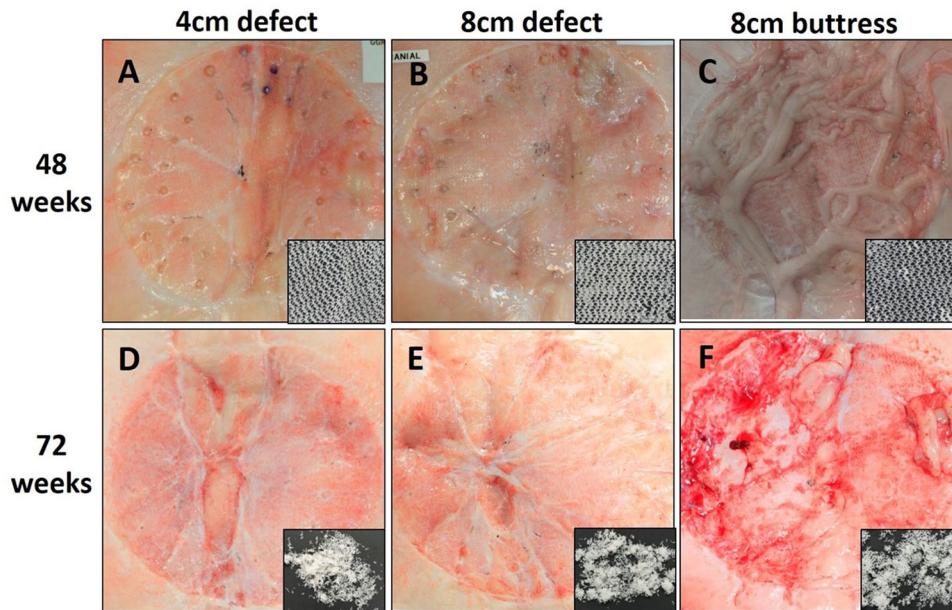
Figure 4. Phasix™ ST Mesh at 48 weeks (*top row*) and 72 weeks (*bottom row*) postimplantation. Inset photos depict Phasix™ ST Mesh after collagenase digestion of adherent native tissue. Phasix™ ST Mesh remained intact at 48 weeks, but only low molecular weight fragments remained at 72 weeks.
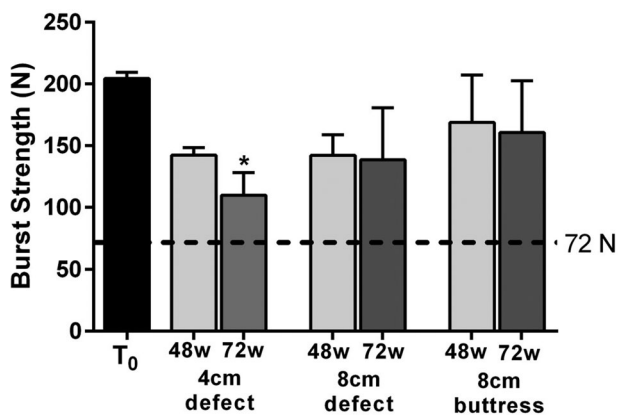

Figure 5. Ball burst strengths of Phasix™ ST Mesh-repaired sites (mean ± standard error of the mean). Dashed line represents Deeken-Matthews recommended 72 N strength threshold [13] (*$p < 0.05$ relative to T_0).
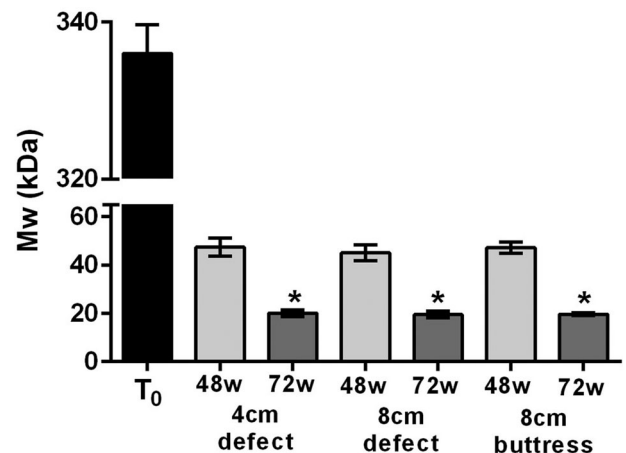

Figure 6. Molecular weight (mean ± standard deviation) of explanted Phasix™ ST Mesh compared to non-implanted (T_0) samples (*$p < 0.05$ relative to T_0).

and 20 ± 0.6 kDa for the 4 cm defect, 8 cm defect, and 8 cm buttress groups, respectively. No significant differences were observed between treatment groups at either time point ($p > 0.05$ in all cases). However, molecular weight was significantly reduced at 72 weeks postimplantation relative to the T_0 molecular weight of Phasix™ ST Mesh (336 ± 3.7 kDa), $p < 0.001$ in all cases. At each time point the standard deviation was very narrow, and the polydispersity values (*data not shown*) did not change substantially, indicating that the P4HB polymer comprising the Phasix™ ST Mesh degraded uniformly throughout the polymer.

Histological evaluation

All components of the Phasix™ ST Mesh were examined histologically, including segments of the mesh overlying the surgical defect, and segments of the mesh to the left and right of the defect. Based on Hematoxylin & Eosin (H&E), Masson's Trichrome (MT), and Picrosirius Red (PSR)

stained slides, the histological appearance of the tissue surrounding the mesh overlying the surgically created defect were comparable among different groups regardless of the time point (Figure 7) and were also similar to the histological appearance of the tissues surrounding the mesh to the left and right of the defect (Figure 8), without any statistically significant differences (Table 2, $p > 0.05$). The tissues surrounding and encasing all segments of the mesh were consistent with an overall predominantly mature and orderly arrangement of collagen/fibrovascular tissue around and within the Phasix™ ST Mesh interstices, including the segment of mesh overlying the defect. Mesh-associated inflammation was in the minimal/slightly detectable range (median score: 1.00, Table 2), comparable among all treated groups regardless of time point, and consistent with inflammation expected for an implanted device evaluated at 48 and 72 weeks postoperatively. The inflammatory response was heterogeneous, consisting of macrophages, lymphocytes, giant cells, and some eosinophils (not always present) across
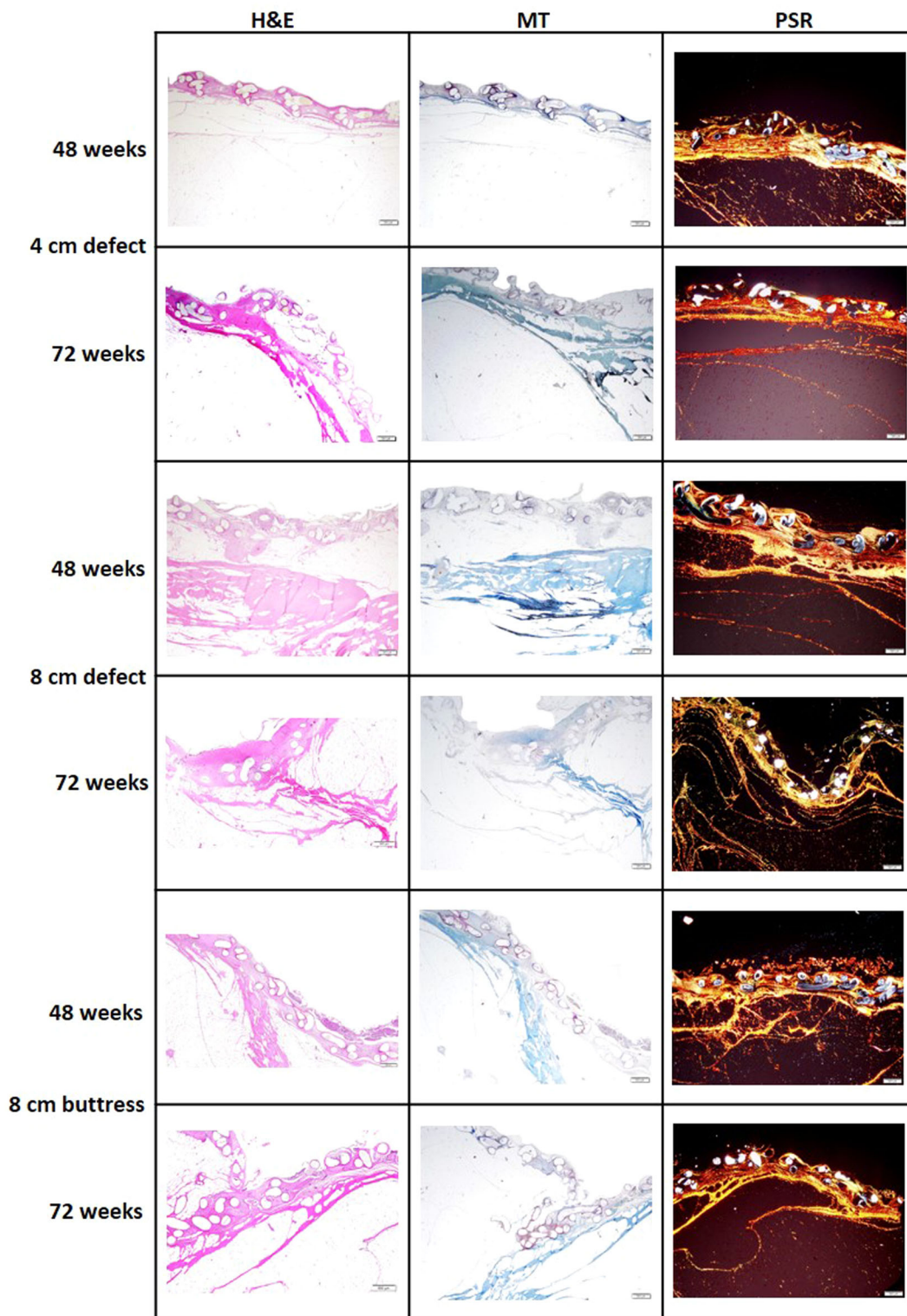
Figure 7. Hematoxylin & Eosin (H&E), Masson's Trichrome (MT), and Picrosirius Red (PSR) stained slides of Phasix^TM ST Mesh-repaired sites at 48 and 72 weeks postimplantation, taken from the center of the defect (scale bar = 500 μm). For a given defect size and time point depicted in a single row, all three images were taken from the same tissue block derived from a single animal. Local tissue response was histologically comparable between groups, regardless of defect type/length and time point. H&E slides show minimal mesh-associated inflammation, consisting of macrophages, lymphocytes, and giant cells, with few eosinophils. MT slides demonstrate mature and well organized fibrotic (collagen) and fibrovascular tissue around and within all segments of the Phasix^TM ST Mesh interstices, including the segment of the mesh overlying the defect. PSR slides depict predominantly mature, type I collagen (red-orange) with minimal immature, type III collagen (green).
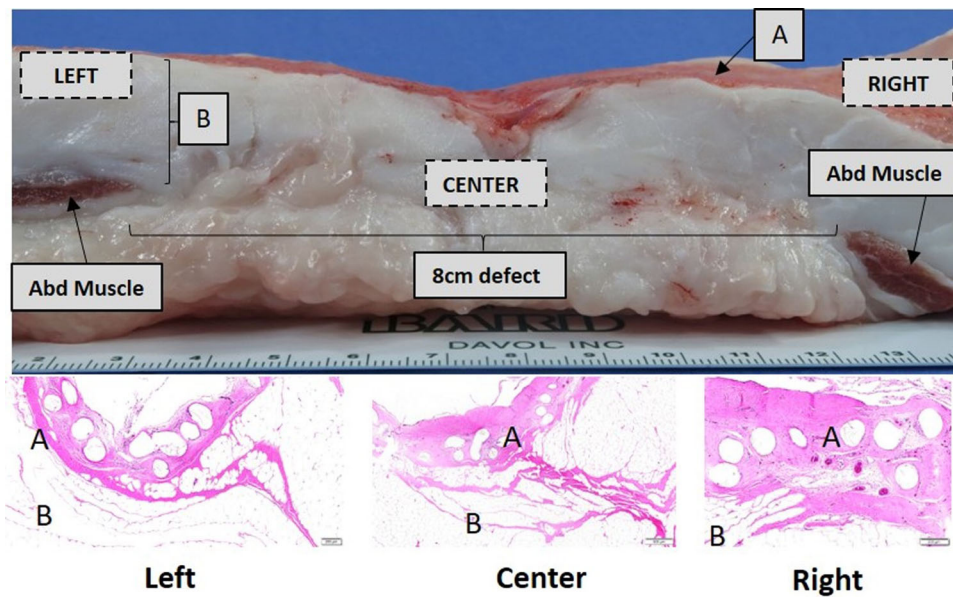
Figure 8. Hematoxylin & Eosin (H&E) stained slides obtained to the left, center, and right of the 8 cm unclosed defect site (72 weeks postimplantation). The left, center, and right locations denoted in the top panel indicate the approximate location of the slides displayed in the bottom panel; A = Mesh/Peritoneal Surface, B = Preperitoneal Fat and Abd Muscle = Abdominal Muscle. Comparable mature collagen/fibrovascular tissue was observed around and within the Phasix™ ST Mesh interstices, including the segment of mesh overlying the defect.

Table 2. Median scores for key histomorphological parameters: Inflammation, fibrosis, neovascularization, and collagen morphology shown for all three defect types and both time points.

Median score	4cm defect						8cm defect						8cm buttress					
	48 weeks			72 weeks			48 weeks			72 weeks			48 weeks			72 weeks		
	L	C	R	L	C	R	L	C	R	L	C	R	L	C	R	L	C	R
Inflammation	1.0	1.0	1.0	1.0	1.0	1.0	1.0	1.0	1.0	1.0	1.0	1.0	1.0	1.0	1.0	1.0	1.0	1.0
Fibrosis	1.0	1.0	1.0	2.0	2.0	2.0	1.0	1.0	1.0	2.0	1.0	1.5	1.0	1.0	1.0	2.0	2.0	2.0
Neovascularization	2.0	2.0	2.0	2.0	2.0	2.0	2.0	2.0	2.0	2.0	2.0	2.0	2.0	2.0	2.0	2.0	2.0	2.0
Collagen Morphology	3.0	3.0	3.0	3.0	3.0	3.0	3.0	3.0	3.0	3.0	3.0	3.0	3.0	3.0	3.0	3.0	3.0	3.0

L: evaluated to the left of the defect, **C**: evaluated in the central area overlying the defect, and **R**: evaluated to the right of the defect.

all treatment groups and time points. Neutrophils, foam cells, and granulomas were not observed in any of the specimens. Vascular integration and neovascularization were mild/slightly detectable and comparable among all treatment groups regardless of time point. Fibrosis and collagen deposition were minimal/barely detectable to mild/slightly detectable in all groups. No evidence of hemorrhage or necrosis was observed in any of the specimens.

Discussion

The objective of this study was to compare the mechanical and histological properties of Phasix™ ST Mesh in various defect sizes and characterize the tissue replacing Phasix™ ST Mesh in a porcine model of ventral hernia repair.

GPC analysis of explanted Phasix™ ST Mesh revealed a significant decrease in molecular weight from 336 kDa at preimplantation (T_0) to 20 kDa at 72 weeks post-implantation for all three groups evaluated ($\sim$94% reduction). No significant differences were observed due to size or type of defect (i.e., 4 or 8 cm, closed or unclosed defects). Macroscopic images of explanted Phasix™ ST Mesh showed only fragments of P4HB fibers remaining at 72 weeks post-implantation. Taken together, these data indicate near complete degradation of Phasix™ ST Mesh by 72 weeks

postimplantation. However, the mechanical strength of Phasix™ ST Mesh-repaired sites (range: 110–169 N) remained stable throughout the course of the study with no significant differences observed between the various treatment groups and time points. At both time points evaluated, all of the Phasix™ ST Mesh-repaired sites exceeded the 72 N threshold previously suggested by Deeken & Matthews for hernia repair applications [13]. Newly-deposited host collagen is likely responsible for the high burst strengths observed for Phasix™ ST Mesh-repaired sites, despite resorption and fragmentation of the P4HB fibers comprising the mesh. Histological analysis confirmed these results with predominantly mature and orderly collagen/fibrovascular tissue observed around and within the Phasix™ ST Mesh interstices, including the segment overlying the hernia defects. The inflammatory response was heterogeneous and consistent with mild inflammation expected of an implanted device at 48 and 72 weeks postimplantation.

The results of this study compare well with several previous studies of Phasix™ Mesh. Martin *et al.* previously reported mechanics, GPC, and histology data at 8, 16, 32, 48, and 72 weeks postimplantation for Phasix™ Mesh implanted in a porcine model [10]. (It should be noted that the Phasix™ Mesh utilized in the Martin study did not contain the ST coating found on the Phasix™ ST Mesh utilized

Table 3. Comparison of measured ball burst and molecular weight data with predicted mesh and host tissue contributions.

Time (Weeks)	Defect type	Measured ball burst strength (N)	M_w (kDa)	Predicted mesh contribution to burst strength N (%)	Predicted host tissue contribution to burst strength N (%)
0	Unimplanted mesh only	204.6	336	220 (100)	0 (0)
48	4 cm unclosed defect	142.4	47	12 (8.4)	130.4 (91.6)
48	8 cm unclosed defect	142.3	45	10 (7.0)	132.3 (93.0)
48	8 cm buttress	168.8	47	12 (7.1)	156.8 (92.9)
72	4 cm unclosed defect	110.0	20	0 (0)	110.0 (100)
72	8 cm unclosed defect	138.6	20	0 (0)	138.6 (100)
72	8 cm buttress	160.6	20	0 (0)	160.6 (100)

in the current study.) In the Martin study, a 2.54 cm defect was surgically created, repaired, and buttressed with Phasix™ Mesh in a retromuscular/preperitoneal (sublay) fashion. GPC analysis showed molecular weights of 56 kDa and 23 kDa at 48 and 72 weeks postimplantation, respectively, which compare well to the current study values of 45–47 kDa at 48 weeks and 20 kDa at 72 weeks postimplantation. Martin also observed macroscopic degradation at 48 weeks postimplantation with only P4HB fragments remaining at 72 weeks postimplantation similar to the current Phasix™ ST Mesh study. Despite these observations of significant P4HB degradation, the ball burst strengths of Phasix™ Mesh-repaired sites remained high at 363 N and 290 N at 48 and 72 weeks postimplantation, respectively and comparable to the strength of the native porcine abdominal wall. It should be noted that the intact peritoneum contributed to the high ball burst values. (The peritoneum was removed prior to mechanical testing in the current Phasix™ ST Mesh study.) Additionally, the Martin porcine model utilized a 2.54 cm defect, which was much smaller than the 4 and 8 cm defects in the current Phasix™ ST Mesh study. When *in vitro* and *in vivo* data were combined, Martin et al. showed that Phasix™ Mesh contributed an estimated 48% to the overall repair strength at 32 weeks, approximately 17% at 48 weeks, and 0% at 72 weeks postimplantation, while the remainder of the repair strength was attributed to host tissue deposition and remodeling of the defect site.

In another study, Deeken et al. reported mechanics, GPC, and histology for Phasix™ Mesh at 6, 12, 26, and 52 weeks postimplantation when a 3 cm defect was surgically created and bridged with Phasix™ Mesh or Phasix™ Plug [9]. (Again, it should be noted that the Phasix™ Mesh utilized in the Deeken study did not contain the ST coating found on the Phasix™ ST Mesh utilized in the current study.) In the Deeken study, the molecular weight decreased significantly over time to 44 kDa at 52 weeks postimplantation (comparable to the current Phasix™ ST Mesh study values of 45-47 kDa at 48 weeks postimplantation). However, the mechanics of the repair site remained stable over time (range: 218–294 N) and significantly stronger ($p < 0.05$) than the native abdominal wall. These data indicate that Phasix™ Mesh augmented the strength of the porcine abdominal wall at all time points investigated, despite significant resorption ($p < 0.05$) of the P4HB fibers. These results are likely explained by the deposition of mature host collagenous tissue at the repair sites, which contributed to the overall repair strength. Similar to the Martin study, the ball burst values for the Deeken study were higher than those observed in the current Phasix™ ST Mesh study. This is likely explained by differences in the tissue plane where the mesh was implanted (i.e preperitoneal versus intraperitoneal) as well as the larger defects utilized in the current study (i.e. 4 and 8 cm defects versus 3 cm defects).

The greatest clinical concern associated with the use of bioresorbable mesh is whether the repair is robust enough to prevent a recurrence after the mesh has been fully resorbed. Immediately after implantation, the mesh provides 100% of the repair strength, as the host tissue has not yet begun to remodel the defect site. As documented in this study, at 48 weeks postimplantation, Phasix™ ST Mesh remained intact. However, utilizing the Martin et al. in vitro data, it is estimated that Phasix™ ST Mesh contributed only 7–8% to the overall repair strength at 48 weeks postimplantation (Table 3). By 72 weeks postimplantation, Phasix™ ST Mesh was completely fragmented, contributing essentially 0% to the overall repair strength. Although the results of this study cannot be translated directly to humans, this study clearly demonstrates that the strength of the repair may persist after the degradation of the P4HB fibers and remains greater than the suggested 72 N threshold for hernia repair applications even at 72 weeks postimplantation.

Conclusion

Phasix™ ST Mesh-repaired sites exhibited mechanical strengths exceeding the recommended 72 N threshold with similar local tissue response regardless of the defect type (unclosed vs. buttressed), defect length (4 cm vs. 8 cm), mesh segment (overlying defect vs. right/left of defect), or time point (48 weeks vs. 72 weeks) in this porcine model of hernia repair.

Prior presentation of data

This study was presented as a poster at the Abdominal Wall Reconstruction conference held in Washington, DC in June 2018.

Funding

Disclosure of interest

Dr. Deeken is the owner of Covalent Bio LLC, which received consulting fees from BD for this project, as well as other, unrelated projects. Mrs. Gagne and Dr. Badhwar are employees of BD.

Author contributions

Study conception and design: Gagne, Badhwar. Acquisition of data: Deeken, Gagne, Badhwar. Analysis and interpretation of data: Deeken, Badhwar. Drafting of manuscript: Deeken, Badhwar. Critical revision: Deeken, Gagne, Badhwar. Final approval of the version submitted for publication: Deeken, Gagne, Badhwar.

Mesh contribution to overall repair site ball burst strength was obtained using the measured molecular weight data and the Martin *et al. in vitro* data to predict mesh contribution [10].

ORCID

Corey R. Deeken ⓘ http://orcid.org/0000-0002-5722-4473

References

1. Cole P. The filigree operation for inguinal hernia repair. *Br J Surg.* 1941;29(114):168–181. doi:10.1002/bjs.18002911403.
2. Koontz AR. Preliminary report on the use of tantalum mesh in the repair of ventral hernias. *Ann Surg.* 1948;127(5):1079–1085. doi:10.1097/00000658-194805000-00026.
3. Usher FC, Ochsner J, Tuttle L, Jr. Use of marlex mesh in the repair of incisional hernias. *Am Surg.* 1958;24(12):969–974.
4. Deeken CR, Lake SP. Fundamentals of prosthetic characteristics. In: Davis D, Bates A, eds. *The SAGES Manual of Hernia Surgery.* Springer Science; 2018: 35–55.
5. Deeken CR, Lake SP. Mechanical properties of the abdominal wall and biomaterials utilized for hernia repair. *J Mech Behav Biomed Mater.* 2017;74:411–427. doi:10.1016/j.jmbbm.2017.05.008.
6. *Instructions for Use—Phasix ST Mesh.* Warwick, RI: C. R. Bard, Inc., accessed electronically 2017.
7. Scott JR, Deeken CR, Martindale RG, Rosen MJ. Evaluation of a fully absorbable poly-4-hydroxybutyrate/absorbable barrier composite mesh in a porcine model of ventral hernia repair. *Surg Endosc.* 2016;30(9):3691–3701. doi:10.1007/s00464-016-5057-9.
8. C. R. Bard ID. *Instructions for Use—SorbaFix Absorbable Fixation System.* Warwick, RI: C R Bard, Inc, accessed electronically 2018.
9. Deeken CR, Matthews BD. Characterization of the mechanical strength, resorption properties, and histologic characteristics of a fully absorbable material (poly-4-hydroxybutyrate-PHASIX Mesh) in a porcine model of hernia repair. *ISRN Surg.* 2013;2013(238067):1–12. doi:10.1155/2013/238067.
10. Martin DP, Badhwar A, Shah DV, et al. Characterization of poly-4-hydroxybutyrate mesh for hernia repair applications. *J Surg Res.* 2013;184(2):766–773. doi:10.1016/j.jss.2013.03.044.
11. Deeken CR, Matthews BD. Comparison of contracture, adhesion, tissue ingrowth, and histologic response characteristics of permanent and absorbable barrier meshes in a porcine model of laparoscopic ventral hernia repair. *Hernia.* 2012;16(1):69–76. doi:10.1007/s10029-011-0854-5.
12. Deeken CR, Matthews BD. Ventralight ST and SorbaFix versus Physiomesh and Securestrap in a porcine model. *JSLS.* 2013;17(4):549–559. doi:10.4293/108680813X13693422520125.
13. Deeken CR, Abdo MS, Frisella MM, Matthews BD. Physicomechanical evaluation of absorbable and nonabsorbable barrier composite meshes for laparoscopic ventral hernia repair. *Surg Endosc.* 2011;25(5):1541–1552. doi:10.1007/s00464-010-1432-0.